Contract No:

This document was prepared in conjunction with work accomplished under Contract No. 89303321CEM000080 with the U.S. Department of Energy (DOE) Office of Environmental Management (EM).

Disclaimer:

SRNL-STI-2023-00035

Proceedings of the ASME 2023
Pressure Vessels & Piping Conference
PVP2023
July 16-21, 2023, Atlanta, Georgia, USA

PVP2023-106637

DETERMINING BURST STRENGTH OF THIN AND THICK-WALLED PRESSURE VESSELS THROUGH PARAMETRIC FINITE ELEMENT ANALYSIS

William R. Johnson, Xian-Kui Zhu, Robert Sindelar, Bruce Wiersma

Savannah River National Laboratory, Aiken SC

ABSTRACT

Previous work on pressure vessel burst strength established a numerical technique for determining the Zhu-Leis burst strength from the pressure-von Mises stress curve provided by finite element analyses (FEA). That work was not developed to capture the burst strength for thick-walled pipes. Recent analytical developments have resulted in a thick-walled Zhu-Leis burst strength solution. In this work we examine this solution and show how it can be determined numerically from FEA models. To determine the Zhu-Leis burst pressure the stress was measured at multiple points through the thickness of the PV as it was pressurized and compared to the analytical thick-walled solution to determine the best measurement location through the thickness. To further examine the burst pressure we developed a parametric code, using the Abaqus Python application programming interface, to rapidly iterate over 60 different combinations of geometries and material properties. This code also extracted pressure and stress data from the results and analyzed the resulting pressure-von Mises stress curves to find the critical point corresponding to the Zhu-Leis burst pressure. A linear recursion was developed which can very accurately predict the PV burst pressure. This regression applies over a range of pipeline steels from grade B to X80, and thicknesses spanning D/t ratios from 6 to 120.

Keywords: linear regression, burst strength, pressure vessel, finite element analysis, pipeline, strength theory

NOMENCLATURE

P_b	burst pressure
P_{zl}	Zhu-Leis burst pressure
$\hat{p}$	normalized burst pressure
D_{m_o}	mean starting diameter
t_o	initial thickness
D_o	outer diameter
D_i	inner diameter
σ_y	yield stress
σ_{uts}	engineering ultimate tensile strength
$\left(\sigma_{eq}^{M}\right)_c$	critical equivalent von Mises stress
ϵ	logarithmic strain
n	strain hardening exponent
K	material strength coefficient
C	burst strength model coefficient
e	Euler's number
E	Young's modulus

1. INTRODUCTION

The accurate determination of pressure vessel (PV) burst strength is critical to making design choices for PVs and linepipes. There has been much research addressing this particular issue. For example, Law and Bowie compared 23 separate methods for the burst pressure prediction of thin-walled pipes [1] while Christopher et. al. compared 12 methods for the burst pressure prediction of thin and thick-walled pipes [2]. These methods have a variety of different characteristics, such as the heuristic limit-load techniques described in references [3] and [4], empirically derived curve fits as in reference [5], hybrid empirical/analytical approaches, as in Svennson's model [6], or fully analytical models, as in Zhu and Leis approach [7].

The derivation of these models usually begins by assuming either the Tresca or von Mises failure criteria for the constitutive material [8]. The Tresca failure theory provides a lower bound prediction, while the von Mises failure theory provides an upper bound prediction. The results of Tresca based theories tend to be overly conservative, while the results of von Mises based theories tend to be too liberal. To address this issue Zhu and Leis developed the average shear stress burst pressure, also known as the Zhu-Leis burst pressure [9] [7]. This failure criterion predicts the average of what the Tresca and von Mises failure criteria predict and has been shown in multiple studies to provide a very accurate prediction of the burst pressure for isotropic power-law hardening materials [1] [8] [10] [11].

Alternatively, finite element analysis (FEA) is often used to predict the burst pressure for damaged PVs or unique geometric configurations. For example, references [12] – [15] used FEA to

predict the burst pressure of corroded pipelines. Typically, a modified RIKS type analysis, which is used for predicting plastic instability, is used for this particular problem. In most commonly used FEA codes, the modified RIKS analysis enforces the von Mises failure criterion, meaning that for perfect PVs FEA predicts the same burst pressure as the analytical von Mises failure criterion. This suggests that for damaged pipelines or unique geometries FEA models will also overpredict the burst pressure. However, reference [7] demonstrates a technique to calculate other theories' burst pressure from FEA derived data using a comparison between the theory's theoretical prediction and the von Mises theoretical prediction.

There are fewer theories available for predicting the burst pressure of thick-walled PVs. Some models include Faupel's formulae, validated using experimental test data [16], and Svennson's approximate formulae [6]. Ihn and Nguyen evaluated these and other formulae against FEA models of pressurized water reactor cooling components and found that their burst strength predictions could vary by as much as 45% [17]. Recently, in reference [18], the Zhu-Leis theory using the average shear stress to predict pressure vessels was extended to thick-walled PV's as well, providing the first analytical theory capable of accurately predicting the burst pressure for both thin and thick-walled PVs.

The purpose of this paper is to develop a technique to calculate the thick-walled Zhu-Leis burst pressure from FEA results. Zhu et. al. showed that if the mean diameter is used instead of the outside diameter (which is typically used) for thin and thick-walled PVs, the Zhu-Leis thick-walled theory predicts the burst pressure with similar accuracy to the thin-walled theory [18]. This is explored herein using python code to generate a database of FEA derived PV burst predictions for different geometries and materials. A curve fit will is derived based on the FEA data, which can predict the burst pressure as a function of both geometric and material properties.

2. THEORETICAL MODELS OF BURST PRESSURE

2.1 Thin-Walled Pressure Vessel Theoretical Models

Typically burst pressure models assume that PV burst pressure depends on the ultimate tensile strength (UTS), the size (specifically D/t ratio), and the plastic flow, defined by n, the strain hardening exponent. Zhu and Leis developed a unified PV burst theory that clarifies the differences between predictions of models based on the Tresca, von Mises, and average shear stress theories [7, 9]. This theory gives that

$$P_b = \left(\frac{C}{2}\right)^{n+1} \frac{4t_o}{D_{m_0}} \sigma_{uts} \tag{1}$$

where σ_{uts} is the ultimate tensile strength, D_{m_o} is the mean starting diameter, t_o is the starting thickness, P_b is the burst strength, and

$$C = \begin{cases} 1 & \text{Tresca Theory} \\ \frac{2}{\sqrt{3}} & \text{Von Mises Theory} \\ \frac{1}{2} + \frac{1}{\sqrt{3}} & \text{Zhu} - \text{Leis Theory} \end{cases} \tag{2}$$

Although not obvious from Eqs. (1) and (2), the Tresca theory provides a lower bound on burst strength, the von Mises theory provides an upper bound, and the Zhu-Leis theory provides an average of the two.

Each of the theories' burst pressure – stress curve can be calculated using the equations

$$P = \frac{1}{d}\left(\frac{C}{2}\right)^{n+1} \left(\frac{e}{n}\ln d\right)^n \frac{4t_o}{D_{m_0}} \sigma_{uts} \tag{3}$$

$$\sigma_{eq} = C^n \left(\frac{e}{2n}\ln d\right)^n \sigma_{uts} \tag{4}$$

where both equations are functions of the ratio $d = (D_m/t)/(D_{m_o}/t_o)$, and e is Euler's number. The burst pressure in Eq. (3) occurs when $P = P_b$ given in Eq. (1).

2.2 Thick-Walled Pressure Vessels Theoretical Models

Svennson derived semi-empircal formulae for the burst pressure of thick vessels based on fundamental mechanics incorporating empirically derived curve fits of the strain-hardening exponent [6]. Svennson's formula for thick walled PVs is

$$P_b = \left(\frac{0.25}{n + 0.227}\right)\left(\frac{e}{n}\right)^n \sigma_{uts} \ln\left(\frac{D_o}{D_i}\right) \tag{5}$$

where D_i is the inner diameter (ID) and D_o is the outer diameter (OD) of the PV. This theory is based on the von Mises theory of plasticity and would thus be expected to provide an upper bound on the burst pressure.

The Zhu-Leis model for thick-walled PV's is given as [18]

$$P_{zl} = 2\left(\frac{C}{2}\right)^{n+1} \sigma_{uts} \ln\left(\frac{D_o}{D_i}\right). \tag{6}$$

Eq. (6) is similar to Eq. (1), except that the geometric dependence occurs as the $\ln D_o/D_i$ as in Eq. (5). This equation is valid for both thin and thick walls.

2.3 Zhu-Leis Burst Pressure Determination Using FEA Von Mises Failure Criterion

The average shear stress and corresponding Zhu-Leis burst pressure provide a more accurate prediction of burst pressure than the von Mises or Tresca solutions. However, most commercial FEA software uses the von Mises flow theory of plasticity, resulting in the von Mises burst pressure solution when analyzing burst pressure models. Reference [7] demonstrates a technique to calculate the Zhu-Leis burst pressure from typical FEA softwares using the critical point, given as

$$\left(\sigma_{eq}^{M}\right)_c = (0.797n^2 - 0.417n + 0.932)\sigma_{uts} \quad (7)$$

where $\left(\sigma_{eq}^{M}\right)_c$ is the critical equivalent von Mises stress that corresponds to the Zhu-Leis burst pressure. When the von Mises stress reaches the $\left(\sigma_{eq}^{M}\right)_c$ calculated value for the material the corresponding pressure in the FEA model is the Zhu-Leis burst pressure of the PV.

3. FINITE ELEMENT SIMULATIONS OF THICK-WALLED PRESSURE VESSELS

Finite element models were developed using Abaqus for all simulations described herein. Large deformation, along with isotropic elastic-plastic strain hardening, was assumed for all models.

3.1 FEA Material Model

The FEA power law hardening is specified with the true stress-strain curve

$$\sigma = \begin{cases} E\varepsilon, & \sigma < \sigma_{ys} \\ K\varepsilon^n, & x \geq \sigma_{ys} \end{cases} \quad (8)$$

with

$$K = \left(\frac{e}{n}\right)^n \sigma_{uts}. \quad (9)$$

The variables in Eqs. (8) and (9) include σ_{ys}, the yield stress, E, the Young's modulus, σ, the true stress, and ϵ the logarithmic or true strain, with K as the strength coefficient and n as the power law hardening exponent. For the models, pipeline steels including grade B up to X80 were used, spanning low to high grade steels often used in practice. Table 1 shows the specific materials and their defining properties.

ABAQUS was used to perform the elastic-plastic FEA simulations using a static Riks step. The Riks type analysis is used when modeling geometric instability, such as the plastic collapse in this case, enforcing the von Mises flow theory.

TABLE 1: FEA MODEL MATERIAL PROPERTIES.

	E (psi)	ν	σ_{ys} (ksi)	σ_{uts} (ksi)	n
Gr. B	30e6	0.3	35.5	60.2	0.192
X52	30e6	0.3	52.2	66.7	0.111
X65	30e6	0.3	65.3	77.6	0.089
X70	30e6	0.3	70.3	82.7	0.085
X80	30e6	0.3	80.5	90.6	0.068

3.2 FEA Geometric Model

Because this work is concerned only with defect free pipelines, a 2D plane-strain quarter model of a pipe is sufficient to capture the behavior of interest. In cases with defects or corrosion this would be insufficient and a 3D model would be used. The geometry and mesh are shown in Fig. 1, along with the symmetry boundary conditions, the internal pressure loading, and stress measurement locations at the ID, mean diameter (MD), and OD. This model, modified for different geometries and materials, was used for all the analyses presented here.

3.3 Failure Criterion for Determining Burst Pressure

As an example of the different failure criteria discussed in Sec. 2, this section presents burst pressure results for models with $D_o/t_o = 10.7$ and 21.3 for a pipeline composed of X65 pipeline steel. Figure 2 compares the FEA predicted burst pressure response to the burst pressure predicted using Eqs. (2) – (4) and (6) for the thick-walled $D_o/t_o = 10.7$ case. As can be seen, the FEA predicted response is almost identical to the von Mises theory predicted burst pressure, as previously described. Figure

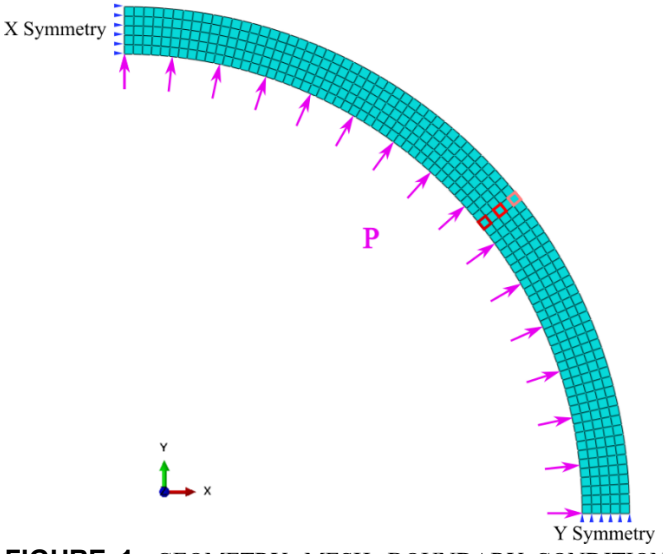

FIGURE 1: GEOMETRY, MESH, BOUNDARY CONDITIONS, AND LOADING, FOR THE FEA PLANE STRAIN PV WITH MEASUREMENT LOCATIONS AT THE ID, MD, AND OD HIGHLIGHTED IN DARK RED, RED, AND PINK RESPECTIVELY, FOR THE $D_o/t_o = 21.3$ CASE.

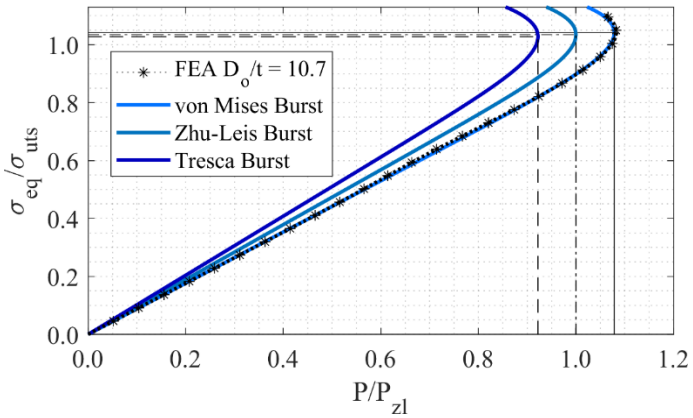

FIGURE 2: COMPARISON OF FEA MODEL AND ANALYTICAL SOLUTION BURST PREDICTIONS FOR $D_o/t_o = 10.7$.

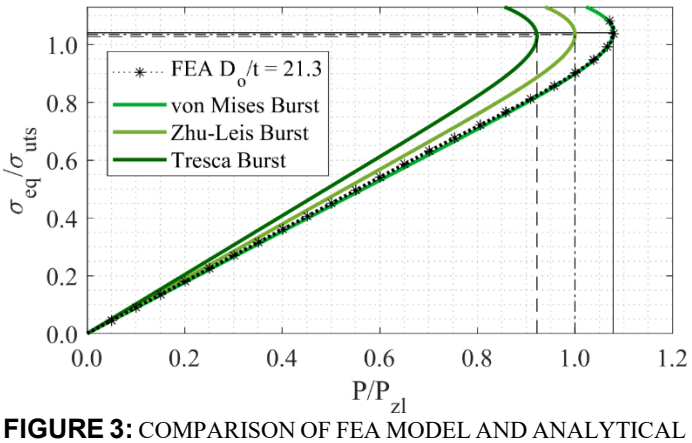

FIGURE 3: COMPOMPARISON OF FEA MODEL AND ANALYTICAL SOLUTION BURST PREDICTIONS FOR $D_o/t_o = 21.3$.

3 compares the FEA predicted burst pressure response to the burst pressure predicted using Eqs. (2) – (4) and (6) for the intermediate $D_o/t_o = 21.3$ case, showing similar results. In Figs. 2 and 3 the pressures were normalized by P_{zl} to demonstrate how they compared to the Zhu-Leis burst pressure. Table 2 shows the three different predicted burst pressures, with the Tresca providing a lower bound, the von Mises an upper bound, and the Zhu-Leis providing the average of the two.

TABLE 2: COMPARISON OF THE BURST PRESSURES (IN KSI) PREDICTED BY THE DIFFERENT THEORIES FOR THE $D_o/t_o = 10.7$ AND 21.3 CASES.

	Tresca	Zhu-Leis	Von Mises
$D_o/t = 10.7$	15.1	16.4	17.7
$D_o/t_o = 21.3$	7.2	7.8	8.4

3.4 Thick-Wall Effect on FEA Simulations

The derivation of Eq. (7) was developed for thin-walled PVs and made the typical thin-walled assumption that the hoop stress was uniformly distributed through the wall thickness. This assumption is invalid for thick-walled PVs. As a result, the best measurement location through the thickness needed to be investigated. Figures 4 and 5 show the von Mises stress at the ID, MD, and ODs for $D_o/t_o = 21.3$ and $D_o/t_o = 10.7$, respectively. For the thin-walled case shown in Fig. 4 the similarity in the pressure-stress curves show a negligible difference between these measurement locations. However, the thick-walled $D_o/t_o = 10.7$ case shows much larger variation during the elastic loading. The ID, MD, and OD pressure-stress curves start to converge as plastic yielding occurs.

Table 3 compares the ID, MD, and OD graphically determined critical stresses from Figs. 4 and 5 to the predicted critical stress using Eq. (7). The difference for the three locations, for the $D_o/t_o = 21.3$ case, was less than 1%, confirming that the thin-walled uniform stress distribution assumption is valid and that the measurement location through the thickness is irrelevant. However, for the $D_o/t_o = 10.7$ case the difference between the predicted critical stress at the ID and OD are 1.4% and 2.3% respectively. The MD predicted stress was approximately 0.5% different from the critical point stress, suggesting that the Zhu-Leis burst pressure can be predicted accurately for thick-walled PVs by measuring the stress at the MD and using Eq. (7) originally developed for thin-walled PVs. For all other simulations shown herein, the stress was measured at the MD.

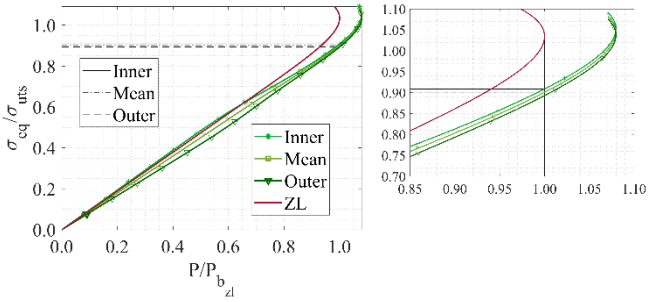

FIGURE 4: COMPARISON OF $D_o/t_o = 21.3$ FEA CALCULATED STRESS AT THE ID, MD, AND OD AS SHOWN IN FIG. 1, DEMONSTRATING THE CURVES' INTERSECTION AT THE CRITICAL POINT FOR THE ANALYTICAL ZHU-LEIS (ZL) AVERAGE SHEAR STRESS PREDICTED PRESSURE-STRESS CURVE (BLACK DASHED AND SOLID LINES), WITH DETAILED VIEW.

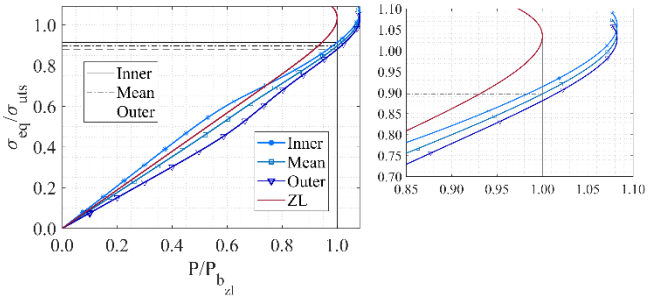

FIGURE 5: COMPARISON OF $D_o/t_o = 10.7$ FEA CALCULATED STRESS AT THE ID, MD, AND OD AS SHOWN IN FIG. 1, DEMONSTRATING THE CURVES' INTERSECTION AT THE CRICITICAL POINT FOR THE ANALYTICAL ZHU-LEIS (ZL) AVERAGE SHEAR STRESS PREDICTED PRESSURE-STRESS CURVE (BLACK DASHED AND SOLID LINES), WITH DETAILED VIEW.

TABLE 3: ID, MD, AND OD COMPARISON OF THE VON MISES STRESSES OF THE PV TO THE PREDICTED CRITICAL POINT STRESS (EQ. (7)) FOR THE ZL THEORY PREDICTED BURST PRESSURE, WITH $(\sigma_{eq}^{M})_c$, ID, MD, AND OD COLUMNS IN KSI.

$\frac{D_o}{t_o}$	$(\sigma_{eq}^{M})_c$	ID	% Diff.	MD	% Diff.	OD	% Diff.
10.7	69.9	70.9	1.4	69.6	0.5	68.3	2.3
21.3	69.9	70.5	0.9	69.9	0.03	69.3	0.9

3.5 Parametric Finite Element Study

Using the material model described in Sec. 3.1 and the geometric model described in Sec. 3.2, a study of the burst pressure of 12 different PV geometries using each of the

materials provided in Table 1 was conducted. The geometries are described in Table 4, and range from $D_o/t_o = 8$ to $D_o/t_o = 120$, which includes both thick and thin-walled PVs. The combination of different geometries and materials resulted in 60 different models. To rapidly iterate over these models and extract burst pressure data the ABAQUS Python application programming interface was used. The Python script was used to automate the generation of new geometry, modify the PV material, extract the burst pressure data, and iterate over all the models.

Figure 6 presents a diagram of the Python and Matlab scripts used to generate and postprocess the FEA models. For the Python script the initial inputs of material and geometry are provided in Table 1 and Table 4, respectively. For each permutation of material and geometry the script does the following:

1. Generates the geometry and material properties.
2. Makes material assignments, creates the mesh, and specifies the analysis.
3. Generates the assembly, loads, and boundary conditions, and creates the element set at the inner and mean diameter for extracting the pressure and stress histories from the output file.
4. Runs the model, and then extracts and saves the pressure and stress data to a text file.
5. Repeats steps 1 – 4 for each combination of material and geometry.

After the models, calculations, and data extractions completed, a MATLAB script would then postprocess the data. The MATLAB script analyzed the data by:

1. Importing it and then plotting the pressure-stress curve.

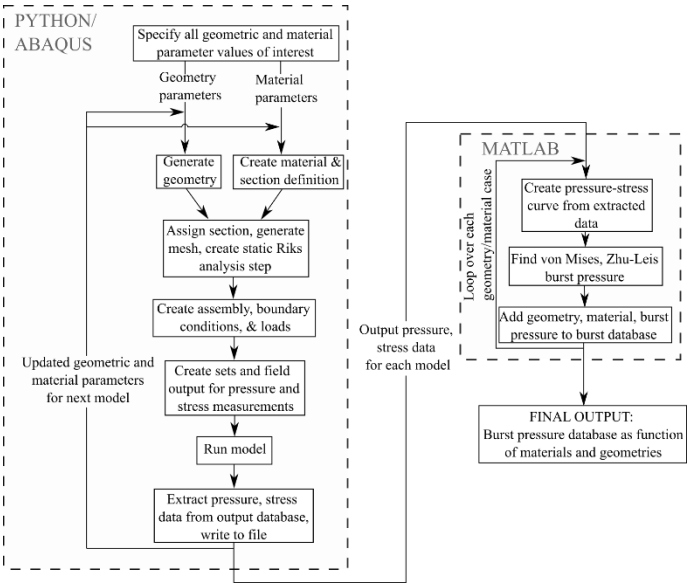

FIGURE 6: PYTHON AND MATLAB SCRIPT DIAGRAM TO GENERATE FEA MODELS, EXTRACT DATA, AND CREATE A BURST PRESSURE DATABASE AS A FUNCTION OF MATERIALS AND GEOMETRIES.

2. Calculating the von Mises and Zhu-Leis burst pressures. These were then checked using figures similar to Figs. 2 and 3 to verify correct performance of the algorithm.
3. Appending the burst pressure and material and geometric parameters to the database.
4. For each pair of material and geometric parameters repeating steps 1 – 3.

The Python and MATLAB script completed output was a database containing the predicted burst pressures for the 60 selected PV material and geometric pairings. After completion of the scripts the simulations and data extraction took approximately 2 hours. This process could be used to create very large databases or for rapid model generation. For this study 60 models were sufficient.

TABLE 4: PV STUDY GEOMETRIC CONFIGURATIONS.

Case No.	Diameter (in)	Thickness (in)	D_o/t_o
1	8	1	8
2	8	0.75	10.7
3	8	0.5	16
4	16	0.75	21.3
5	16	0.5	32
6	24	1	24
7	24	0.5	48
8	24	0.25	96
9	30	0.75	40
10	30	0.5	60
11	30	0.25	120
12	42	0.5	84

3.6 FEA Burst Pressure Curve Fit

There are a variety of ways in which the FEA burst pressure database could be analyzed. A regression model of the burst pressure as a function of the three input variables n, D/t, and the UTS could be attempted. The difficulty of a three-variable regression makes this approach less likely to provide a meaningful interpolation of the data. Instead, by applying an effective normalization the number of regression variables can be reduced to a manageable amount. In reference [7], for the development of the average shear stress thin-walled burst pressure Zhu and Leis normalized burst pressure data using the thin-walled Tresca strength solution, causing the normalized burst data to reduce to a function of n only. This suggests that, because this work is looking at the thick-walled solution, normalizing by the thick-walled Tresca strength solution, provided in reference [19] as $P_t = \sigma_{uts} \ln (D_o/D_i)$ would be an effective choice. Figure 7 shows that the FEA extracted data, normalized using this value reduces to be a linear function of n, as expected.

The linearity of the data suggests that a linear regression would provide an effective prediction of the burst strength for both thin and thick-walled PVs across this broad range of strain-

hardening exponents. The regressive relationship found from this data is

$$\hat{p}(n) = 1.079 - 0.6395n \quad (10)$$

where

$$\hat{p} = \frac{P_b}{\sigma_{uts} \ln\left(\frac{D_o}{D_i}\right)}. \quad (11)$$

The regression provided in Eq. (10) combined with the normalization provided in Eq. (11) gives a burst pressure relationship of

$$P_b(n, \sigma_{uts}, D_o, D_i) = (1.079 - 0.6395n)\sigma_{uts} \ln\left(\frac{D_o}{D_i}\right) \quad (12)$$

In Fig. 7 the normalized FEA burst pressure data falls within a very narrow bounding envelope, highlighted in yellow, with the maximum difference being less than 0.5% across all material and geometric parameters used. The small amount of error in the linear regression and the data it was developed on suggests that Eq. (12) would accurately predict the burst pressure across the entire range of materials from grade B to X80 steels and geometric cross-sections, from $D/t = 8$ to $D/t = 120$.

To further highlight the significance of the choice in normalization, Fig. 8 displays the same FEA data, normalized using the thin-walled Tresca strength solution $P_T = \sigma_{uts} 2t_0/D_0$. Using this normalization there is very wide scatter, highlighted in yellow, caused by the wide range of D_o/t_o ratios. This confirms the unsuitability of the thin-walled Tresca burst solution for the normalization of the thick-walled burst pressure.

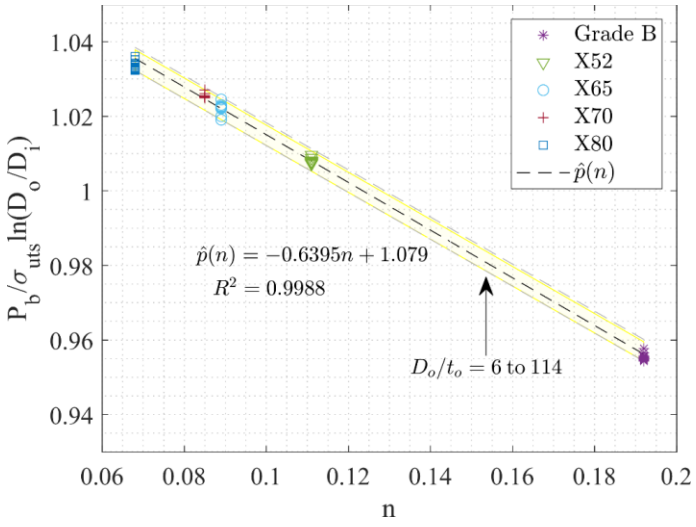

FIGURE 7: BURST PRESSURE NORMALIZED BY THE THICK-WALLED TRESCA SOLUTION, AS A FUNCTION OF THE STRAIN HARDENING EXPONENT N FOR ALL 60 DATA POINTS FROM THE PARAMETRIC STUDY, ALONG WITH LINEAR INTERPOLATION $\hat{p}(n)$ AND BOUNDING ENVELOPE (DASHED GRAY LINES).

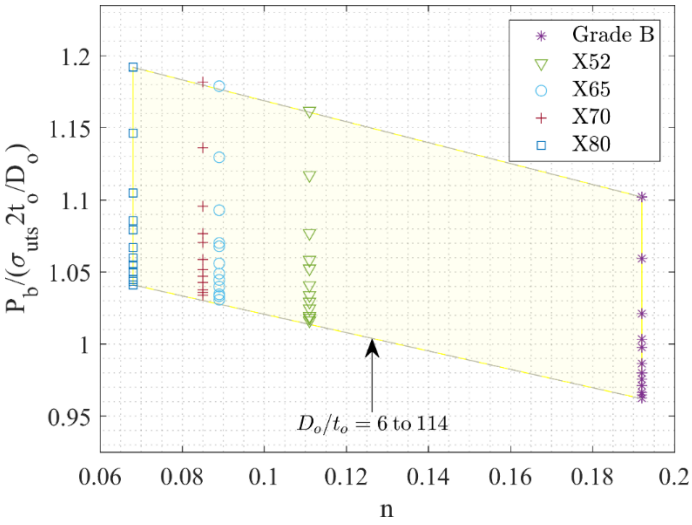

FIGURE 8: BURST PRESSURE NORMALIZED BY THE THIN-WALLED TRESCA SOLUTION FOR ALL 60 DATA POINTS FROM THE PARAMETRIC STUDY AS A FUNCTION OF THE STRAIN HARDENING EXPONENT N, ALONG WITH BOUNDING ENVELOPE (DASHED GRAY LINES).

4. VALIDATION OF PROPOSED BURST STRENGTH MODEL

4.1 Comparison with FEA Results

To evaluate the effectiveness of the model in Eq. (10), Table 5 shows a comparison of model predictions with the FEA predictions for the lowest and highest grade steels examined, Grade B and X80, for several D/t ratios spanning the range from 8 to 120. The burst pressure data provided from the FEA models give the approximate Zhu-Leis burst pressure. This was also compared to the Svensson model, provided in Eq. (5), because it is the most often used of the thick-walled burst pressure models. In order to provide a comparison, the percent error between the FEA, Eq. (10) model, and the Svensson model, are also provided.

The percent error between the proposed model and the FEA burst strength shows that there is less than 1% error over the material and geometric range examined. The error between the Svennson and FEA predictions ranges between approximately 4% for the Grade B steel and 6 percent for the X80 steel. For both models, as the wall thickness increased the error also increased. The overprediction of the Svennson model observed in Table 5 is a result of this model assuming the von Mises flow theory of plasticity. The low percent error of the regression burst model demonstrates that Eq. (10) very closely captures the relationship between the PV burst pressure and its constitutive material and geometry.

4.2 Comparison with Full-Scale Burst Data

Figure 9 provides more rigorous validation by comparing the Eq. (10) burst pressure prediction to full scale burst data. This experimentally derived burst data was obtained from a number of sources (see references [20] – [31]). The data in the sources

TABLE 5: BURST PRESSURE PREDICTION COMPARISON OF EQ. (10) TO THE SVENNSON (EQ. (5)) AND FEA ZHU-LEIS PREDICTIONS.

Mat	OD (in)	WT (in)	FEA (psi)	Eq 10 (psi)	% Er	Eq 5 (psi)	% Er
GrB	42	0.50	1388	1387	0.03	1440	3.8
GrB	30	0.25	968	967	0.03	1004	3.8
GrB	24	0.50	2451	2450	0.03	2543	3.8
GrB	16	0.75	5664	5667	0.04	5881	3.8
GrB	8	0.75	11916	11953	0.31	12406	4.1
GrB	8	1.00	16453	16560	0.65	17188	4.5
X80	42	0.50	2255	2261	0.26	2378	5.4
X80	30	0.25	1573	1577	0.26	1658	5.4
X80	24	0.50	3982	3993	0.27	4199	5.5
X80	16	0.75	9204	9235	0.34	9713	5.5
X80	8	0.75	19361	19480	0.61	20487	5.8
X80	8	1.00	26738	26990	0.94	28384	6.2

cover a geometric range similar to that used for the FEA study, including burst pressures with pipelines ranging from $D_o/t_o =$ 6 to 114, and strain hardening exponents ranging from approximately 0.025 to 0.17. Thick-walled PV burst pressure data is indicated by filled markers. This figure is an updated version of Fig. 6 in reference [9] employing the thick-walled normalization. It demonstrates that the new model in Eq. (10) provides predictions very close to the analytical Zhu-Leis burst pressure and gives the average between the von Mises and Tresca

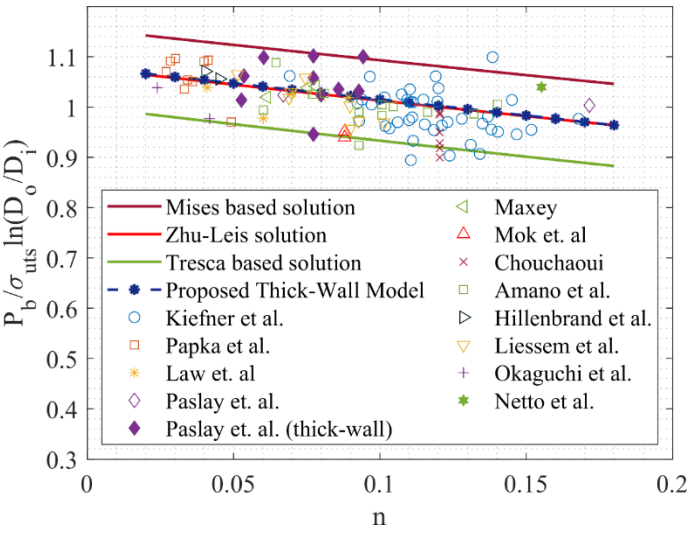

FIGURE 9: PROPOSED MODEL COMPARISON TO THE THEORIES DESCRIBED IN EQS. (2) AND (5) AND FULL-SCALE REFERENCE DATA.

burst solutions, giving confidence that the model provides accurate PV burst pressure prediction over many different materials and geometries.

5. CONCLUSIONS

This study demonstrated a scripting technique to generate a large number of models and rapidly extract data from them. It was used to develop a semi-analytical model of PV burst strength that is valid over a wide range of geometries and materials commonly used in pipeline steels, including both thick and thin-walled PVs. The main outcomes include a demonstration that:

1) The effect of the measurement location through the PV wall thickness matters for thick-walled PVs and that the mean diameter is a more accurate measurement location for the stresses and strains, for predicting burst pressure.
2) PV burst pressure FEA databases can be quickly constructed from a large number of models using ABAQUS Python scripts to cover a wide range of key parameters using the architecture shown in Fig. 4.
3) Numerical and experimental validation confirmed that the burst pressure model presented herein accurately predicts thick and thin-walled PV burst pressure for many line pipe steels and frequently used geometric configurations.

ACKNOWLEDGEMENTS

The authors are grateful for the financial support from the Department of Energy and its Laboratory Directed Research and Development (LDRD) program through the LDRD Project 2022-00077 at Savannah River National Laboratory.

REFERENCES

[1] M. Law and G. Bowie, "Prediction of failure strain and burst pressure in high yield-to-tensile strength ratio linepipe," *International Journal of Pressure Vessels and Piping,* vol. 84, pp. 487-492, 2007.

[2] T. Cristopher, B. Rama Sarma, P. Govindan Potti, B. Nageswara Rao and K. Sankarnarayanasamy, "A comparative study on failure of pressure estimations of unflawed cylindrical vessels," *International Journal of Pressure Vessels and Piping,* vol. 79, pp. 53 - 66, 2002.

[3] M. Muscat, D. Mackenzie and R. Hamilton, "A work criterion for plastic collapse," *International Journal of Pressure Vessels and Piping,* vol. 80, pp. 49-58, 2003.

[4] M. F. Shi and J. C. Gerdeen, "Effect of strain gradient and curvature on forming limit diagrams for anisotropic sheets," *Journal of Materials Shaping Technology,* vol. 9, pp. 253-268, 1991.

[5] D. H. Oh, J. Race, S. Oterkus and E. Chang, "A new methodology for the prediction of burst pressure for API 5L X grade flawless pipelines," Ocean Engineering, vol. 212, p. 107602, 2020.

[6] N. L. Svensson, "The bursting pressure of cylindrical and spherical vessels," *Journal of Applied Mechanics,* vol. 25, pp. 89-96, 1958.
[7] X.-K. Zhu and B. N. Leis, "Theoretical and numerical predictions of burst pressure of pipelines," *Journal of Pressure Vessel Technology,* vol. 129, pp. 644-652, 2007.
[8] X.-K. Zhu and B. N. Leis, "Evaluation of burst pressure prediction models for line pipes," *International Journal of Pressure Vessels and Piping,* vol. 89, pp. 85-97, 2012.
[9] X.-K. Zhu and B. N. Leis, "Average shear stress yield criterion and its application to plastic collapse analysis of pipelines," *International Journal of Pressure Vessels and Piping,* vol. 83, pp. 663-671, 2006.
[10] J. Yang and S. Hu, "Estimation of burst pressure of PVC pipe using average shear stress yield criterion: Experimental and numerical studies," Applied Sciences, vol. 11, p. 10477, 2021.
[11] M. Sun, Y. Chen, H. Zhao and X. Li, "Analysis of the impact factor of burst capacity models for defect-free pipelines," International Journal of Pressure Vessels and Piping, vol. 200, p. 104805, 2022.
[12] A. Karstensen, A. Smith and S. Smith, "Corrosion damage assessment and burst test validation of 8in X52 linepipe," in *Proceedings of ASME Pressure Vessel and Piping Conference*, Atlanta, GA, 2001.
[13] B. Fu and M. Kirkwood, "Determination of failure pressure of corroded linepipes using the nonlinear finite element method," in *Proceedings of the Second International Pipeline Technology Conference, Vol. II*, Ostend, Belgium, 1995.
[14] J. B. Choi, B. K. Goo, J. C. Kim, Y. J. Kim and W. S. Kim, "Development of limit load solutions for corroded gas piplines," *International Journal of Pressure Vessels and Piping,* vol. 80, pp. 121 - 128, 2003.
[15] H. C. Phan, A. S. Dhar and B. C. Mondal, "Revisiting burst pressure models for corroded pipelines," *Canadian Journal of Civil Engineering,* vol. 44, no. 7, pp. 485-494, 2017.
[16] J. H. Faupel, "Yield and bursting characteristics of heavy-wall cylinders," Transactions of the American Society of Mechanical Engineers, vol. 78, no. 5, pp. 1031 - 1061, 1956.
[17] N. Ihn and H. G. Nguyen, "Investigation of burst pressures in PWR primary pressure boundary components," Nuclear Engineering and Technology, vol. 48, pp. 236-245, 2016.
[18] X.-K. Zhu, B. Wiersma, R. Sindelar and W. R. Johnson, "New strength theory and its application to determine burst pressure of thick-wall pressure vessels," in *Proceedings of the ASME 2022 Pressure Vessels & Piping Conference*, Las Vegas, NV, 2022.
[19] L. B. Turner, "The stresses in a thick hollow cylinder subjected to internal pressure," *Transactions of Cambridge Philosophical Society,* vol. 21, pp. 377-396, 1910.
[20] J. Kiefner, W. Maxey and A. Duffy, "The significance of the yield-to-ultimate strength ratio of line pipe materials. Summary report to Pipeline Research Committee," American Gas Association, 1971.
[21] S. Papka, J. Stevens, M. Macia, D. Fairchild and C. Petersen, "Full-size testing and analysis of X120 linepipe," *International Journal of Offshore and Polar Engineering,* vol. 14, pp. 42-51, 2004.
[22] M. Law, G. Bowie and L. Fletcher, "Pipeline behaviour, the hydrostatic strength test, and failure strain," in *Proceedings of the 15th Conference of PRCI and EPRG Pipeline Conference*, Orlando FL, 2005.
[23] P. Paslay, E. Cernocky and R. Wink, "Burst pressure prediction on thin-walled, ductile tubulars subjected to axial load," in *Proceedings of Applied Technology Workshop on Risk Based Design of Well Cashing and Tubing*, Woodlands, TX, 1998.
[24] W. Maxey, "Y/T significance in line pipe," in *Proccedings of the seventh symposium on line pipe research*, Houston, TX, 1986.
[25] D. Mok, R. Pick, A. Glover and R. Hoff, "Bursting of line pipe with long external corrosion," *International Journal of Pressure Vessels and Piping,* vol. 46, pp. 195-216, 1991.
[26] B. Chouchaoui, Evaluating the remaining strength of corroded pipelines, Departhment of Mechanical Engineering, University of Waterloo Canada, 1993.
[27] K. Amano, M. Matsuoka, T. Ishihara, K. Tanaka, T. Inoue, Y. Kawaguchi and M. Tsukamoto, "Significance of yield ratio limitation to plastic deformation of pipeline in high pressure proof test," in Proceedings of the seventh symposium on line pipe research, Houston TX, 1986.
[28] H. Hillenbrand, A. Liessem, G. Knauf, K. Niederhoff and J. Bauer, "Development of large-diameter pipe in grade X100," in *Proceedings of the Third International Conference of Pipeline Technology*, Brugge, Belgium, 2000.
[29] A. Liessem, M. Graef, G. Knauf and U. Marewski, "Influence of thermal treatment on mechanical properties of UOE linepipe," in 4th International Conference on Pipeline Technology, Ostend, Belgium, 2004.
[30] S. Okaguchi, H. Makino, M. Hamada, A. Yamamoto, T. Ikeda, I. Takeuchi, D. Fairchild, M. Macia, S. Papka, J. Stevens, C. Petersen, J. Koo, N. Bangaru and M. Luton, "Development and mechanical properties of X120 linepipe," International Journal of Offshore Polar Engineering, vol. 14, 2004.
[31] T. Netto, U. Ferraz and S. Estefen, "The effect of corrosion defects on the burst pressure of pipelines," *Journal of Constructional Steel Research,* vol. 61, pp. 1185-1204, 2005.